ELSEVIER

Biophysical Chemistry 106 (2003) 241–252

Biophysical Chemistry

www.elsevier.com/locate/bpc

Kinetic characterization of TAR RNA–Tat peptide and neomycin interactions by acoustic wave biosensor

Nardos Tassew, Michael Thompson*

Department of Chemistry, University of Toronto, 80 St. George Street, Toronto, ON, Canada M5S, 3H6

Received 3 February 2003; received in revised form 22 May 2003; accepted 28 May 2003

Abstract

The kinetics of binding of short Tat peptides and an aminoglycoside molecule to the human immunodeficiency virus-type 1(HIV-1) TAR RNA and to a bulge mutant analogue (MTAR) is studied in a biosensor format by monitoring the time course of the response in a series resonance frequency, using an acoustic wave biosensor. Association and dissociation rate constants are evaluated by fitting the experimental data to a simple 1:1 (Langmuir) model. Kinetic rate and equilibrium dissociation constants show that MTAR–peptide complexes are subject to a higher dissociation rate and are less stable compared to the corresponding TAR–peptide complexes. In addition, longer peptides display enhanced discrimination ability than a shorter peptide according to the equilibrium dissociation constants evaluated using this technique. K_D values for TAR–Tat vs. MTAR–Tat complexes are 2.6 vs. 3.8 μM for Tat-12, 0.87 vs. 4.3 μM for Tat-18 and 0.93 vs. 1.6 μM for Tat-20. The equilibrium dissociation constant for TAR–neomycin complex is 12.4 μM and it is comparable to the values obtained from non-biosensor type assays. These findings are in parallel with those cited in the literature and the results from this study underline the potential of the acoustic wave sensor for detailed biophysical analysis of nucleic acid–ligand binding.

Keywords: Acoustic wave biosensor; Binding kinetics; TAR–Tat; Neomycin

1. Introduction

Nucleic acid–protein interactions are routinely characterized by assays that are based on gel-shift and filter binding protocols [1–4]. These techniques, though in wide use for the quantitative assay of bimolecular interactions, are laborious, time-consuming and require one or both molecules to be tagged with a radioisotope or a fluorescent dye. Such techniques provide information about the affinity of the biomolecular interactions and do not give a detailed insight into the kinetics underlying the interaction process. In contrast, detection based on a biosensor eliminates the need for the use of any type of label, and enables rapid measurement of biomolecular interactions in real-time from which important kinetic parameters can be evaluated in addition to the equilibrium constants.

*Corresponding author. Tel.: +1-416-978-3575; fax: +1-416-978-8775.

E-mail address: mikethom@chem.utoronto.ca (M. Thompson).

0301-4622/03/$ - see front matter © 2003 Elsevier Science B.V. All rights reserved.
doi:10.1016/S0301-4622(03)00155-8

Biosensors are being increasingly employed for biochemical and biophysical characterization of nucleic acid–ligand chemistry. Surface plasmon resonance (SPR) is the frontrunner for such applications and it has been the main biosensor technique for determining kinetic rate and equilibrium constants. These include evaluation of DNA hybridization, protein–protein, nucleic acid–protein and small molecular interaction kinetics [5–7]. It has also been shown that the rate and affinity constants obtained from SPR to be equivalent to those determined from solution-based methods such as isothermal calorimetry (ITC) and stopped-flow fluorescence (SFF), if reaction conditions are carefully controlled [8,9]. In contrast there have been only few cases where acoustic wave sensors are used for such applications.

With respect to acoustic wave detection, the thickness-shear mode (TSM) sensor is based on the instigation of ultrasonic waves in piezoelectric materials such as AT-cut quartz. This device, which oscillates at frequencies in the range of a few MHz, propagates transverse shear waves into the surrounding medium to a decay length of the order of micrometers. The response of the TSM sensor in liquids is governed by a number of factors including the viscoelastic, acoustoelectrical and interfacial acoustic coupling properties of a surface-bound film and the surrounding fluid [10,11]. This apparent complexity can be turned to an advantage through incorporation of the device into a network analysis (equivalent circuit) configuration, which generates several parameters such as series resonance frequency (f_s), motional resistance (R_m), inductance (L), and static and motional capacitance (C_s and C_m). The quantity that is commonly employed, is the series resonant frequency, however, a thorough understanding of the above acoustic parameters can yield important information on the structural changes of biomolecules instigated by binding events at the sensor–solution interface. Although employment of the acoustic wave sensor to detect a variety of biochemical systems has been growing in recent years, relatively little attention has been paid to the measurement of the kinetics of reactions involving biochemical species at the sensor–liquid interface. Included in these studies has been the evaluation of the kinetics of DNA duplex formation [12], protein adsorption [13], and in very few cases, the binding of ligands to nucleic acids [14]. It is noteworthy that a number of these investigations were performed using the 'wash–dry' protocol in which the sensor is removed after each binding event, to be followed by washing and drying steps. This method possesses severe disadvantages compared to the real-time monitoring of binding interactions through the use of the flow-injection analysis (FIA) technique. Not only does the wash and dry procedure suffer from poor reproducibility, but there is also a distinct possibility that the intervening drying step could lead to the denaturation of captured nucleic acids in hybridization assays [15].

A typical kinetic experiment on a biosensor involves immobilization of one of the partners, establishment of a baseline sensor response in running buffer, injection of an analyte solution during the association phase, followed by dissociation of the analyte by washing with buffer. Data are presented as a plot of biosensor response vs. time and it is analyzed using a mathematical model. The Langmuir model is commonly employed to describe the kinetics with assumptions that: binding is limited to a monolayer, all sites are equivalent, and binding to one site is independent of the occupancy state of neighbouring sites. Obtaining meaningful kinetic rate and affinity constants from biosensor analysis requires careful control of reaction conditions and sensor design. Some important considerations for obtaining high quality biosensor data are minimization of mass transport effects, avoidance of impure and multivalent analytes and careful control of immobilization chemistry to generate a homogeneous surface [16,17].

As a model system for acoustic wave measurement of biochemical kinetics, we chose to study the interaction between the *trans*-activation responsive region of the HIV-1 mRNA (TAR) and short peptides derived from the regulatory Tat protein and an inhibitor molecule. The HIV-1 Tat protein is a regulatory protein that stimulates transcription of the HIV virus by binding to the *trans*-activation responsive region at the 5′end of mRNA transcripts [18–22]. The protein contains 86 amino acids,

however, the arginine rich basic region (residues 59–72) is sufficient to bind the target RNA. Thus, short peptides containing the binding domain are commonly employed as models to investigate the much larger and more complex TAR–Tat interaction. The bulge structural element is essential for Tat recognition and mutations in this region reduce binding of the protein and transactivation levels in vivo [23–25]. The TAR–Tat interaction is inhibited by aminoglycoside antibiotics, which interact with TAR mainly through electrostatic complementarity with the negatively charged RNA backbone. Neomycin is such molecule and binds to the stem region of TAR and facilitates the dissociation of the peptide by inducing conformational changes in the RNA [26–28].

The kinetics and thermodynamics of binding of a set of short Tat peptides to TAR RNA has been widely studied using gel-shift assay protocols and circular dichroism (CD) spectroscopy [23,29–31]. The researchers have examined the effect of mutations, introduced at specific sites in the basic region of the peptides and the bulge RNA element, on the kinetic and affinity constants of TAR–Tat complexes. They demonstrated that Tat peptides form less stable complexes with MTAR compared to the wild type RNA and that binding affinity is an indicator of the discriminating ability of the peptides between TAR and TAR bulge mutants. In the previous studies, we established that the chemistry of interactions of TAR RNA with Tat peptides and neomycin could effectively be studied using the acoustic wave device [32,33]. In the present article, we describe a kinetic analysis of the interaction of Tat peptides with TAR RNA and a bulge mutant analogue (MTAR), derived from measurements conducted in the FIA mode. Values obtained from such experiments will be compared to those reported in the literature involving the above interactions.

2. Materials and methods

2.1. TAR RNA synthesis

The, A, U, G and C phosphoramadites and the C-biotinTEG controlled-pore glass columns were purchased from Glen Research, Sterling, Virginia. tetrazole/acetonitrile, 1-methyimidazole/tetrahydrofuran, acetic anhydride/pyridine/tetrahydrofuran, iodine/H_2O/pyridine and anhydrous acetonitrile were obtained from Applied Biosystems, Mississauga, ON. Ammonium hydroxide, ethanol, tetrabutylammonium fluoride (TBAF), triethylamine, tetraethylammonium acetate (TEAA), trifluoroacetic acid (TFA), acetonitrile and sterile water were purchased from Sigma Aldrich, Oakville, ON.

2.2. Peptide synthesis

The resins and amino acid residues were purchased from Advanced ChemTech, Louisville, KY. Dimethylformamide, *N*-methylpyrrolidone, piperidine and *O*-(7-Azabenzotriazol-1-yl)-*N*,*N*,*N*′,*N*′-tetramethyluronium hexafluorophosphate (HATU) were obtained from Sigma Aldrich, Oakville, ON.

2.3. Buffer

One molar Tris HCl (pH 7.5), 5 M NaCl, 0.5 M EDTA were all purchased from Sigma Aldrich, Oakville, ON.

2.4. Neomycin

Neomycin sulfate was purchased from Sigma Aldrich and used without any further treatment.

2.5. Devices

Nine megahertz AT-cut piezoelectric quartz crystals, coated with polished gold electrodes on both sides, were obtained from International Crystal Manufacturing, Oklahoma City, OK.

2.6. Flow cell and network analyzer

The responses of the TSM sensor in liquid was measured using an HP 4195 network/spectrum analyzer (Hewlett-Packard, Palo Alto, CA, USA). The quartz crystal is placed between two halves of a Plexiglas flow cell with o-rings, in such a way that the electrodes are in electrical contact with the network analyzer. Only one face of the crystal is exposed to buffer and sample solutions

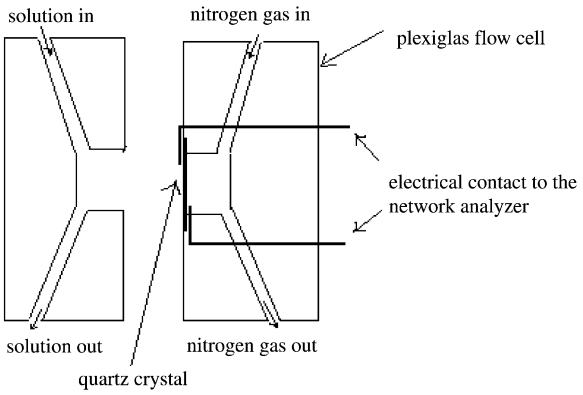

Fig. 1. Schematic of the TSM sensor flow cell assembly. AT-cut quartz crystal is sandwiched between the two-halves of the flow cell. One face of the crystal is exposed to buffer and biochemical solutions while the other face is kept dry under a flowing nitrogen gas.

and the other face is kept dry by a continuously flowing nitrogen gas (Fig. 1). The flow of nitrogen is extremely low (6 ml/min) such that it does not cause noise associated with turbulent flow. Buffer and sample solutions are introduced in a flow-through format using a peristaltic pump (4 channel EVA-pump model 1000). Data are taken every 30 s and the values of the equivalent circuit element of the crystal are calculated internally by the analyzer from measured data. A PC is connected to the analyzer and the frequency response is displayed on the screen in real-time.

2.7. TAR RNA synthesis and characterization

TAR RNA containing 31 bases (5′-GGC CAG AUC UGA GCC UGG GAG CUC UCU GGC C-3′) was chemically synthesized using 2′-*t*-butyldimethylsilyl and 5′-dimethoxytrityl protected phosphoramadites on Applied Biosystem 392 DNA/RNA synthesizer. Biotin was incorporated at the 3′ end during the synthesis. The oligoribonucleotide was desalted and detritylated using oligonucleotide purification cartridges (Poly Pak). The molecular mass was confirmed by MALDI-MS. The RNA was dried and stored at −20 °C and it was re-suspended in Tris-buffer (10 mM Tris, 70 mM NaCl, 0.2 mM EDTA) prior to use.

2.8. Tat peptide synthesis

All Tat-peptides were synthesized using standard Fmoc chemistry protocols and were purified by reverse-phase HPLC using a linear gradient from water (0.1% TFA) to 70% acetonitile (0.1% TFA). The mass of the peptides was confirmed by electrospray mass spectrometry. The concentration was determined spectroscopically from the tyrosine absorbance in 6 M guanidine hydrochloride (275.5 nm, $\varepsilon = 1475$) [34].

2.9. RNA–ligand interaction and kinetic analysis

The binding of three synthetic Tat-peptides (Tat-12, Tat-18 and Tat-20) and neomycin to immobilized TAR and MTAR RNA have been investigated (Figs. 2 and 3). All the peptides have the minimum required basic region for binding, with the longer fragments containing more amino acid residues from the carboxy-terminal of the Tat protein. The quartz crystals were cleaned with acetone, ethanol and water, and dried under a stream of nitrogen gas before use. All acoustic wave measurements were taken during a continuous flow, and the pump was only stopped momentarily in order to switch between solutions. The sensor surface is first equilibrated with Tris-buffer before immobilization of RNA. When a stable resonant frequency response is obtained, a 500 μl solution of neutravidin (1 mg/ml in Tris-buffer) is flowed over the sensor surface, followed by wash with buffer for approximately 30 min in order to remove non-adsorbed protein from the surface. The above procedure was carried out at room temperature and a constant flow rate of 60 μl/min. Immobilization of the RNA on the gold surface of the crystals is accomplished using avidin–biotin interactions. Thus, a 500 μl solution of 3′biotinylated TAR RNA (1 μM in Tris-buffer) is injected over the neutravidin-modified surface. Following, a 250 μl solution of Tat peptides (5–50 μM), and neomycin (5–100 μM) is flowed over the RNA-modified surface for approximately 4 min. Dissociation of bound peptide/neomycin is initiated by washing with Tris-buffer that contained a small amount of TAR (0.1 μM) for a duration of 15 min. All binding experiments were carried out at room

(a)

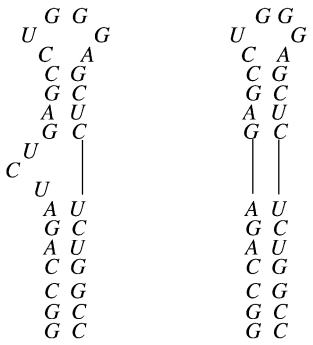

(b)

Tat-12 *Tyr-Gly-Arg-Lys-Lys-Arg-Arg-Gln-Arg-Arg-Arg-Pro*

Tat-18 *Tyr-Gly-Arg-Lys-Lys-Arg-Arg-Gln-Arg-Arg-Arg-Pro-Pro-Gln-Gly-Ser-Gln-Thr*

Tat-20 *Tyr-Gly-Arg-Lys-Lys-Arg-Arg-Gln-Arg-Arg-Arg-Pro-Pro-Gln-Gly-Ser-Gln-Thr-His-Gln*

Fig. 2. (a) Secondary structure of HIV-1 TAR RNA and bulgeless TAR (MTAR), nucleotides G16-C46. (b) Schematic of the primary sequences of Tat-12, Tat-18 and Tat-20 peptides derived from the HIV-1 Tat protein, containing the Arg-rich RNA binding region.

temperature and a constant flow rate of 60 μl/min, except in situations where higher flow rates had to be employed for the purpose of evaluating mass-transport effects.

2.10. Data analysis

Real-time frequency-time data were fitted to an exponential function using the software Origin 6.1.

3. Results and discussion

Biochemical kinetic analysis using biosensors in the FIA format involves immobilization of one of the reactants on the surface of the device. In the present work, the RNA is attached to the surface of the gold electrode of the quartz crystal through neutravidin-biotin chemistry. Neutravidin is a tetrameric protein and a deglycosylated derivative, which displays a similar binding affinity to biotin as the parent molecule, avidin. However, the derivative possesses a much lower isoelectric point (6.2 vs. 10.5) and exhibits less non-specific binding than the parent entity [35]. Previous studies have shown that the structure of avidin is compromised by gold surfaces of low surface free energy (hydrophilic), whereas neutravidin does not exhibit such behavior [33]. The protein is very suitable for the immobilization of biotinylated nucleic acids in a flow-through format since it adsorbs strongly to gold surfaces and forms a mono-layer [36], resulting in a significant frequency change. The neutravidin–biotin interaction is very strong and stable under most conditions ($K_d = 10^{-15}$); thus, the RNA remains attached to the surface during the course

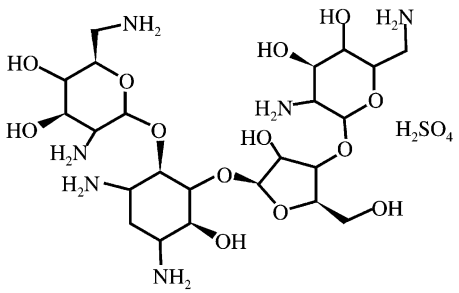

Fig. 3. Structure of neomycin sulfate.

of flow-through experiments. During acoustic wave measurements, a significant series resonance frequency drop confirms the immobilization of the RNA when biotinylated TAR is flowed over the neutravidin-modified surface of the sensor electrode. The frequency does not deviate from the new value despite being subjected to extensive flow-through washing with buffer solution. From radiolabeling studies performed under the same conditions as acoustic wave measurements, the surface RNA loading is estimated to be approximately 1 pmol/cm^2 for 1 μM solution of TAR. It should be noted that the only difference between TAR and MTAR is the bulge region, which is far from the site of attachment of biotin. Thus, it is assumed that the bulge mutation does not affect the degree of immobilization and the surface loading of MTAR for 1 μM solution would be the same as that of TAR. This is further confirmed by the fact that flowing through 1 μM solution of both nucleic acids yields very similar frequency shifts. It is also reasonable to assume that the surface coverage was reproducible in all cases since frequency shifts exhibiting high reproducibility were obtained for immobilization of the RNAs (55 ± 2 Hz, $n = 25$).

The binding of a peptide (analyte, P) to immobilized RNA (R) is a two-step process that requires the transport of analyte to the biosensor surface, followed by binding to the nucleic acid. This process is described by the following equations,

$$P_{\text{bulk}} \underset{k_m}{\overset{k_m}{\rightleftarrows}} P_{\text{surface}} \tag{1}$$

$$P_{\text{surface}} + R \underset{k_d}{\overset{k_a}{\rightleftarrows}} RP \tag{2}$$

where k_a and k_d are the association and dissociation rate constants, respectively. The mass transport term, k_m, is dependent on the diffusion coefficient of the analyte, the flow rate and the geometry of the flow cell. In kinetic measurements, avoidance of mass-transport effects is critical in terms of obtaining the meaningful rate constants. This is especially important in the case of very fast reactions in which the rate of binding is equal or faster than the diffusion of the analyte to the surface. Accordingly, it is necessary to ensure that the interaction is not under diffusion control by using a flow rate of sufficient magnitude in tandem with a surface displaying a low binding capacity. Dissociated analytes must also be transported away from the surface rapidly enough to avoid rebinding. Employing a surface of low binding capacity reduces the depletion rate of the analyte from the interfacial region, and also ensures that rebinding is minimized. It is often assumed that the concentration of the analyte in the proximity of the sensor surface remains constant because of a continuous flow of solution and accordingly the binding to be essentially the same as that of a well-mixed system. This can only be true if the kinetic behaviour is not influenced by mass transport. Otherwise, the mathematical model used to fit the data should incorporate a term for mass transport contributions. The effect of mass transport can be experimentally ruled out by performing the reaction at different flow rates and immobilization densities. An increase in binding rate for a higher surface capacity and flow rate are indications that the reaction is under mass transport limitation.

All the measurements in this work were performed under high flow rates (60 μl/min) and excess amount of peptide in solution to ensure the concentration of peptide in the interfacial region remains the same as that of the bulk. It should also be emphasized that experiments conducted at increased flow rates resulted in no changes in the reaction kinetics and yielded similar rate constants ($k_{\text{on}} = 0.028$, 0.031, 0.029 s^{-1} for 60, 120 and 180 μl/min, respectively) (Fig. 4). Thus, the influence of mass-transport can be excluded and the rate constants can be considered to reflect the actual reaction rate. The experiments were also repeated at least three times to ensure reproducibility.

In the absence of mass-transport limitations, the binding between the immobilized RNA and the peptide in solution is represented by Eq. (2) and the rate of formation of the peptide–RNA complex is given by

$$\frac{\mathrm{d}[RP]}{\mathrm{d}t} = k_a[P][R] - k_d[RP]_t \tag{3}$$

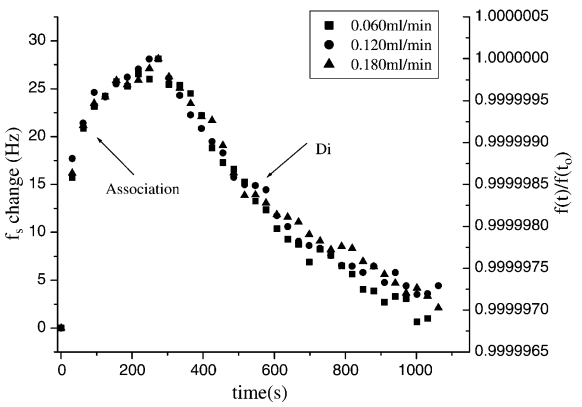

Fig. 4. Frequency–time plots showing reproducibility of the association and dissociation regions for TAR–Tat-20 at different flow rates (60, 120, 180 μl/min).

The concentration of the peptide is much greater than that of the immobilized RNA and remains essentially unchanged during the course of the reaction. Thus, the reaction can be described by pseudo-first order kinetics. The concentration of unbound RNA [*R*] is the difference between the total amount on the surface [R_o] and the amount of complex, $[R]=[R_o]-[RP]$. After substitution, Eq. (3) becomes,

$$\frac{d[RP]}{dt}=k_a[P]\left([R]_o-[RP]_t\right)-k_d[RP]_t \quad (4)$$

The binding of Tat-12, Tat-18 and Tat-20 to immobilized RNA gives rise to a positive frequency change as depicted by a representative plot given in Fig. 5. It has been previously demonstrated through control experiments and radioisotope labeling that the sensor is insensitive to non-specific interactions of peptides with the underlying neutravidin layer and only responds to specific binding events taking place at the sensor–liquid interface [32]. Thus, the change in the frequency signal during the course of the experiment can be used to describe the rates of binding and dissociation of TAR–Tat complexes, and yield kinetic rate constants. Even though the Sauerbrey [37] mass-response model cannot be strictly employed to describe the relationship between frequency and mass when the sensor is employed in solution, it is reasonable to assume that the change in the sensor's response is proportional to the amount of complex formed on the surface, as long as solutions conditions (density, viscosity, conductivity) are kept constant [13,14,38]. At concentrations employed in our experiments, the effect of the above conditions can be considered minimal and does not contribute to the signal [39]. In addition, it has been previously determined that the magnitude of the frequency signal exhibits a direct dependence on the concentration of the peptide solution, up to a concentration of 100 μM, indicating that there is a positive relationship between the frequency and the amount of complex formed on the surface even though mass is not the sole factor in determining the sensor's response [32,40]. Thus, Eq. (4) can be written as:

$$\frac{df}{dt}=k_a[P](f_{max}-f_t)-k_df_t \quad (5)$$

Where the total amount of TAR represents the maximum analyte binding capacity of the surface and is given by f_{max}. Rearranging Eq. (5) gives

$$\frac{df}{dt}=k_a[P]f_{max}-\left(k_a[P]+k_d\right)f_t \quad (6)$$

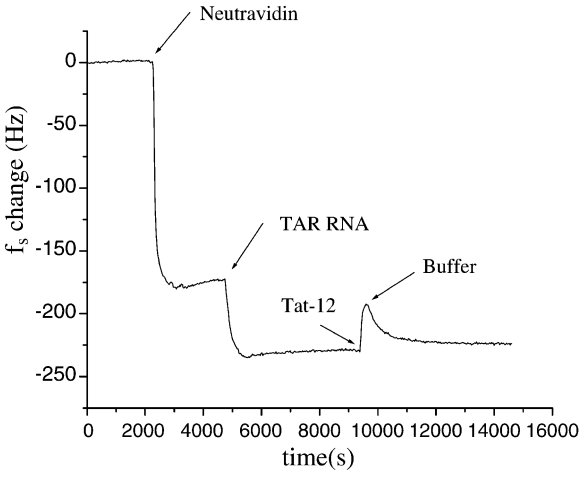

Fig. 5. A representative frequency response plot for the interaction of Tat-12 with immobilized TAR RNA through neutravidin–biotin linkage.

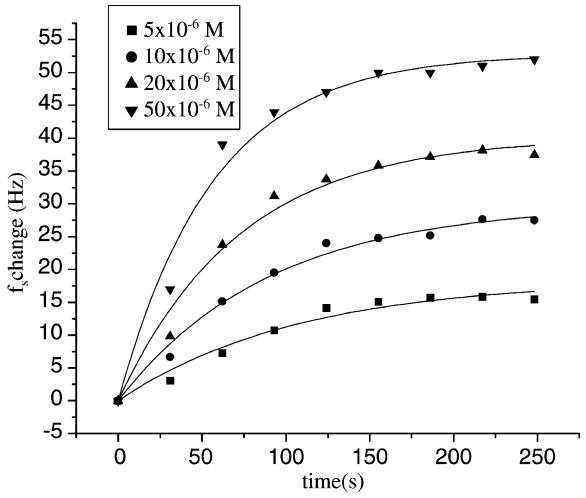

Fig. 6. Frequency response curves for binding of Tat-12 to TAR RNA at different concentrations (5, 10, 20, 50 μM).

Data obtained from the sensor can be divided into association and dissociation regions. Analysis of the association part yields the apparent association rate constant (k_{on}) produced from the individual curve fits, which contains information on both the association and dissociation events and varies with the analyte concentration.

$$k_{on} = k_a[P] + k_d \quad (7)$$

k_{on} can be determined from the slope of df/dt vs. f_t plot in Eq. (6) or by directly fitting frequency-time data from the association part to the integrated form of the equation

$$f_t = f_{max}[1 - \exp(-k_{on}t)] \quad (8)$$

It is more appropriate to determine k_{on} from the integrated equation since linear transformations also transform the parameter-associated errors, no longer reflecting errors in the original data. In addition, the data from many analyte concentrations must be employed in order to derive a single rate constant. In contrast, fitting the integrated rate equation with non-linear regression allows for the determination of k_{on} from a single experiment. A typical association plot for the interaction of Tat-12 with TAR RNA at different concentrations is shown in Fig. 6. Association and dissociation rate constants can be determined from the slope and intercept of the corresponding k_{on} vs. [peptide] plot, respectively.

Table 1
Kinetic rate and equilibrium dissociation constants for TAR–Tat and TAR–neomycin complexes

TAR-ligand	k_a (M^{-1} s^{-1})	k_d (s^{-1})	K_D (μM)
Tat12-TAR	323	0.00085	2.6
Tat12-MTAR	532	0.00201	3.8
Tat18-TAR	497	0.00043	0.87
Tat18-MTAR	262	0.00112	4.3
Tat20-TAR	853	0.00079	0.93
Tat20-MTAR	438	0.00070	1.6
Neomycin	110	0.00137	12.4

The association and dissociation rates along with equilibrium dissociation constants for the interaction of Tat peptides and neomycin with TAR RNA are summarized in Table 1. The K_D constant for TAR/neomycin complex is found to be in the micromolar range from acoustic wave biosensor measurement (Figs. 7 and 8) and compares well with the IC_{50} value determined from mobility shift assays [41]. Dissociation constants for TAR/Tat complexes indicate the stability order to be TAR/Tat12 < TAR/Tat18 and TAR/Tat20. This result is not surprising because, though the arginine-rich

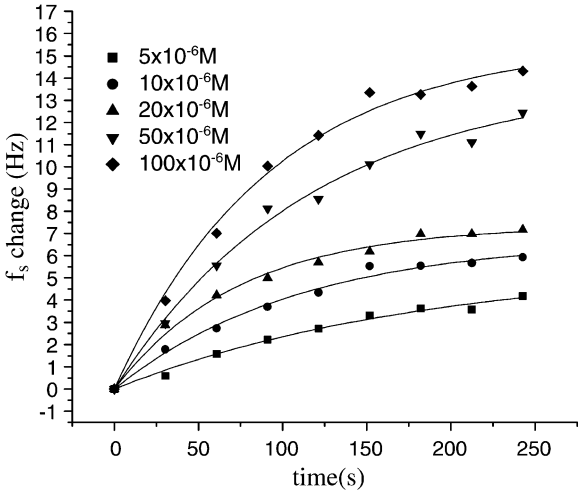

Fig. 7. Frequency response curves for binding of neomycin to TAR RNA at different concentrations (5, 10, 20, 50, 100 μM).

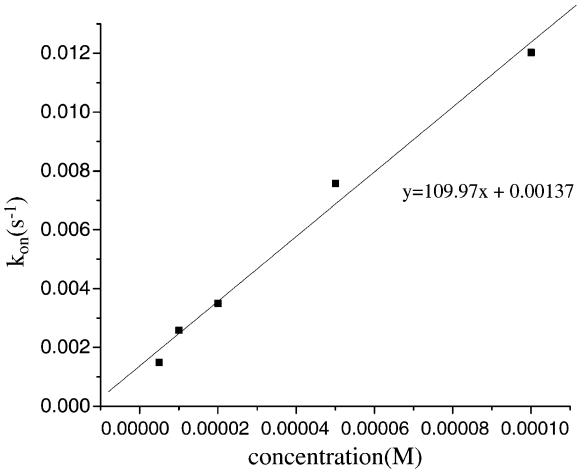

Fig. 8. Plot of k_{on} vs. [neomycin] from which k_a and k_d constants for TAR–neomycin interaction are determined.

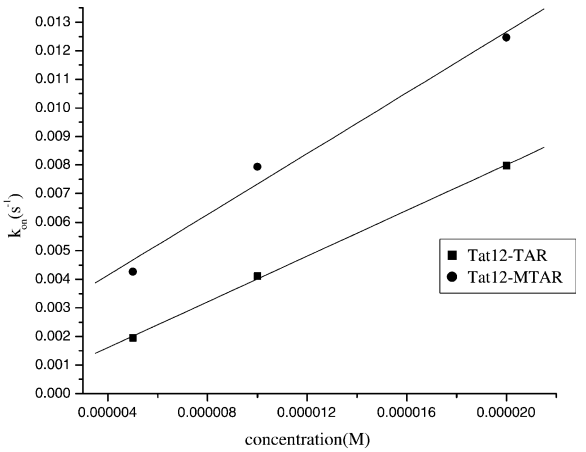

Fig. 9. Plot of k_{on} vs. [peptide] for the interaction of Tat-12 with TAR and MTAR.

region (residues 49–59) in the RNA-binding domain of the Tat protein is sufficient to bind to TAR, other amino acid residues outside this region contribute to the overall binding affinity and kinetic stability of the TAR–Tat complexes. This is the result of added intermolecular interactions due to the inclusion of more amino acid residues, making the complexes more stable. Higher affinities for Tat-18 and Tat-20 are the result of increases in the association rate of the peptides with TAR RNA. However, kinetic stabilities of TAR–Tat-18 and TAR–Tat-20 could not be differentiated from these results, may be due to comparable stability of the two complexes since the difference between the peptides is only two amino acid residues from the C-terminal region.

In general, Tat forms more stable complexes with TAR compared to bulge mutant analogues of the RNA [42]. Chemical interference studies have shown that the bulge region of TAR is critical for binding, and mutations introduced in this region greatly reduce transactivation levels [43]. On close examination of the association and dissociation behaviour of each TAR–peptide and MTAR–peptide complex from acoustic wave sensor data, a number of differences become apparent. The plot of k_{on} vs. [Tat-12] displays similar slopes for interaction of the peptide with both TAR and MTAR, leading to very close association rate constants, which indicates the poor discrimination ability of Tat-12 (Fig. 9). Tat-18 and Tat-20 are better discriminators between wild type and mutant RNA (Figs. 10 and 11). The k_{on} vs. [peptide] plots of these peptides for binding with TAR yield a relatively higher slope compared to the corresponding plots for MTAR, demonstrating that association rates are higher with the former nucleic acid. A small amount of binding of the peptides to the

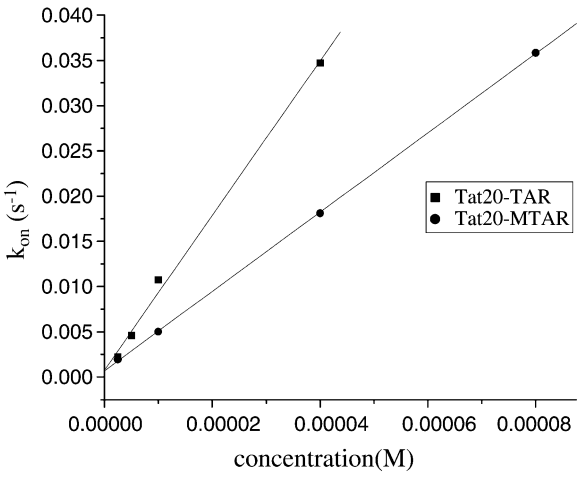

Fig. 10. Plot of k_{on} vs. [peptide] for the interaction of Tat-20 with TAR and MTAR.

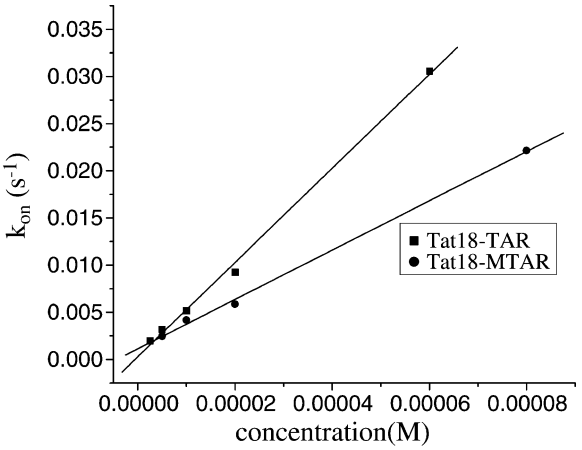

Fig. 11. Plot of k_{on} vs. [peptide] for the interaction of Tat-18 with TAR and MTAR.

mutant RNA is expected in view of the fact that many RNA binding proteins attach weakly to nucleic acid moieties regardless of sequence or structure. However, the discriminating ability of the Tat peptides increases when more amino acid residues are incorporated into the RNA-binding basic region [29]. It has been demonstrated by gel-shift assays that shorter Tat peptides do not discriminate as well as longer ones between TAR and bulge mutants [44] and that there is a good correlation between binding affinity of peptide-TAR complex and the ability of the peptide to distinguish between wild type and mutant RNAs [29]. Thus, the stability of the complex is an important determinant of specificity in RNA–protein interactions. Biological function requires that proteins discriminate relevant RNA targets in the presence of all other non-cognate RNAs in living cells and this arises from the difference in binding energy due to a unique arrangement of intermolecular forces, as well as the ability of the RNA to fold around the protein together with the energetic penalties associated with this process [45–47].

There is significant variability in reported K_D values of TAR/Tat complexes from non-biosensor type assays, ranging from 60 pM to 0.3 μM [48,49]. Equilibrium dissociation constants determined from the TSM sensor are on the higher end of the spectrum when compared to values in the literature. Even though in some cases biosensor measurements yield similar rate constants to those obtained from solution-based methods [15,50], values from the two techniques may not match for several reasons. Immobilization of a biomolecule limits the diffusional and rotational freedom of the molecule and may alter the kinetics and thermodynamics of binding [16,51]. It can also interfere with the binding properties of immobilized molecules by inducing conformational changes in the binding sites or sterically hindering the access of the analyte. In addition, variations could arise from differences in the assay systems and conditions under which the experiments are carried out, such as ionic strength, temperature and pH. However, K_D values of nucleic acid–protein complexes determined employing a biosensor and other type of techniques should reflect the same order of relative stability. In line with this, the results from our measurements are in agreement with what is reported in the literature concerning TAR–Tat interactions and the stability order of the complexes for different Tat peptides. Longer Tat peptides are better discriminators between TAR and bulge mutants and form more stable complexes compared to smaller ones and mutations in the bulge region of TAR reduce the binding affinity of the peptides [23,29,30]. Thus, the acoustic wave biosensor presents an appealing alternative to solution-based techniques since it makes the determination of the kinetics of bimolecular interactions easier and faster. However, the use of the sensor to characterize macromolecular interactions is still very young and there is still much to accomplish in areas such as sensor design and development of mathematical models that adequately describe binding events at the sensor–solution interface.

4. Conclusion

Determination of K_D values by a biosensor-based protocol, such as the one discussed in the present work, offers clear advantages over other solution-based techniques, since reactions that may require several hours for equilibrium to be established, can be assayed within a very short time. In addition, rate constants can also be determined,

which are critical for elucidation of reaction mechanisms in nucleic acid–protein interactions. Both association and dissociation rate constants can be obtained in a matter of few minutes, a factor which presents positive implications for low-to-medium throughput screening technology in the drug-discovery process. Furthermore, with respect to acoustic wave technology, unlike other techniques such as SPR, the physics also offers the possibility to obtain valuable chemical information regarding receptor–ligand chemistry from the various network analysis-based parameters such as series resonance frequency and motional resistance. In terms of the nucleic acid–ligand system described here, the binding of specific peptides to the RNA can be discriminated through the magnitude and direction of change, on binding, of the afore mentioned parameters [32].

Acknowledgments

The authors are very grateful to the Natural Sciences and Engineering Council of Canada for support of this work. They also thank A.G. Woolley, University of Toronto for allowing the use of facilities for peptide synthesis.

References

[1] R.V. Talanian, C.J. McKnight, P.S. Kim, Science 249 (1990) 769–771.
[2] C. Berger, I. Jelesarov, Biochemistry 35 (1996) 14984–14991.
[3] B. Koldin, M. Suckow, Nucl. Acids Res. 23 (1995) 4162–4169.
[4] M. Ueno, M. Sawada, K. Makino, T. Morii, J. Am. Chem. Soc. 116 (1994) 11137–11138.
[5] P.Y. Tsoi, M. Yang, Biochemistry J. 361 (2002) 317–325.
[6] A. Szabo, L. Stolz, R. Granzow, Curr. Opin. Struct. Biol. 5 (1995) 699–705.
[7] A. Sadana, A. Ramakrishnan, Sens. Actuators B 85 (2002) 61–72.
[8] J.E. Ladbury, M.A. Lemmon, M. Zhou, J. Green, M.C. Botfield, Proc. Natl. Acad. Sci. USA 92 (1995) 3199–3203.
[9] W. Ito, Y. Kurosawa, J. Biol. Chem. 268 (1993) 20668–20675.
[10] M.S. Yang, M. Thompson, Anal. Chem. 65 (1993) 3591–3597.
[11] G.L. Hayward, M. Thompson, J. Appl. Phys. 83 (1998) 2194–2201.
[12] Y. Okahata, M. Kawase, K. Niikura, Anal. Chem. 70 (1998) 1288–1296.
[13] Y. Mao, W. Wei, J. Zhang, H. Peng, L. Wu, Microchem. J. 70 (2001) 133–142.
[14] M. Yang, C.M.H. Yang, H.L. Chan, Langmuir 14 (1998) 6121–6129.
[15] R.B. Towery, N.C. Fawcett, P. Zhang, J.A. Evans, Biosens. Bioelectron. 16 (2001) 1–8.
[16] D.G. Myszka, Curr. Opin. Biotech. 8 (1997) 50–57.
[17] T.A. Morton, D.G. Myszka, Method Enzymol. 295 (1998) 268.
[18] B. Berkhout, K.-T. Jeang, Cell 59 (1989) 273–282.
[19] R. Tan, A. Brodsky, J.R. Williamson, A.D. Frankel, Semin. Virol. 8 (1997) 186–193.
[20] K. Watson, R.J. Edwards, Biochem. Pharmacol. 58 (1999) 1521–1528.
[21] J. Tao, L. Chen, A.D. Frankel, Biochemistry 36 (1997) 3491–3495.
[22] F. Hamy, U. Asseline, J. Grasby, S. Iwai, C. Pritchard, G. Slim, et al., J. Mol. Biol. 230 (1993) 111–123.
[23] K.M. Weeks, D.M. Crothers, Cell 66 (1991) 577–588.
[24] K.M. Weeks, D.M. Crothers, Perspect. Drug Discovery Des. 1 (1993) 225–234.
[25] K.M. Weeks, C. Ampe, S.C. Schultz, T.A. Steitz, D.M. Crothers, Science 249 (1990) 1281–1285.
[26] H.Y. Mei, M. Cui, A. Heldsinger, S.M. Lemrow, J.A. Loo, K.A.S. Lowery, et al., Biochemistry 37 (1998) 14204–14212.
[27] F. Hamy, V. Brondani, A. Florsheimer, W. Stark, M.J.J. Blommers, T. Klimkait, Biochemistry 37 (1998) 5086–5095.
[28] S. Wang, P.W. Wuber, M. Cui, A.W. Czarnik, H.Y. Mei, Biochemistry 37 (1998) 5549–5557.
[29] K.S. Long, D.M. Crothers, Biochemistry 34 (1995) 8885–8895.
[30] K.M. Weeks, D.M. Crothers, Biochemistry 31 (1992) 10281–10287.
[31] C. Dingwall, I. Ernberg, M.J. Gait, S.M. Green, S. Heapy, J. Karn, et al., EMBO J. 9 (1990) 4145–4153.
[32] N. Tassew, M. Thompson, Anal. Chem. 74 (2002) 5313–5320.
[33] L.M. Furtado, H. Su, M. Thompson, Anal. Chem. 71 (1999) 1167–1175.
[34] H. Edelhoch, Biochemistry 6 (1967) 1948–1954.
[35] Y. Hiller, J.M. Gershoni, E.A. Bayer, M. Wilchek, Biochem. J. 248 (1987) 167–171.
[36] R.C. Ebersole, J.A. Miller, J.R. Moran, M.D. Ward, J. Am. Chem. Soc. 112 (1990) 3239–3241.
[37] G. Sauerbrey, Z. Physics 155 (1959) 206–222.
[38] Y. Mao, W. Wei, S. Zhang, G. Zheng, Anal. Bioanal. Chem. 373 (2002) 215–221.
[39] H. Su, M. Thompson, Biosens. Bioelectron. 10 (1995) 329–340.
[40] X.C. Zhou, L.Q. Huang, S.F.Y. Li, Biosens. Bioelectron. 16 (2001) 85–95.

[41] H.Y. Mei, D.P. Mack, A.A. Galan, N.S. Halim, A. Heldsinger, J.A. Loo, et al., Bioorg. Med. Chem. 5 (1997) 1173–1184.
[42] B. Lustig, I. Bahar, R.L. Jernigan, Nucl. Acids Res. 26 (1998) 5212–5217.
[43] P. Muchga, A. Szyk, P. Rekowski, J. Barciszewski, J. Chromatogr. A 968 (2002) 211–220.
[44] K.M. Weeks, D.M. Crothers, Biochemistry 31 (1992) 10281–10287.
[45] G. Varani, Acc. Chem. Res. 30 (1997) 189–195.
[46] N. Leulliot, G. Varani, Biochemistry 40 (2001) 7949–7956.
[47] E. Westhof, J. Med. Chem. 42 (1999) 1250–1261.
[48] M.J. Churchur, C. Lamont, F. Hamy, C. Dingwall, S.M. Green, A.D. Lowe, P.J.G. Butler, M.J. Gait, J. Karn, J. Mol. Biol. 230 (1993) 90–110.
[49] K.M. Weeks, D.M. Crothers, Cell 66 (1991) 577–588.
[50] Y.S.N. Day, C.L. Baird, R.L. Rich, D.G. Myszka, Protein Sci. 11 (2002) 1017–1025.
[51] R. Karlsson, H. Roos, L. Fagerstam, B. Persson, Methods 6 (1994) 99–110.